

Capturing of the tsunami wave energy by islands*

An.G. Marchuk

Abstract. The process of capturing wave energy by a round-shaped island with a conical relief for the surrounding bottom is studied in this work. The kinematics of the tsunami wave having initially straight front near such an island was investigated by the method of step-by-step orthogonal advancement of wave front. An estimate was obtained for a part of wave energy that refracted and captured by the bottom slope surrounding the island. Numerical modeling of the same problem was also carried out within the framework of the shallow-water model; this modeling confirmed the results obtained by the kinematic method. The quantitative assessment of the part of wave energy reflected by the island and captured by its conical shelf is in good agreement with the results obtained by kinematical method.

1. Tsunami impact to the conical island

As was shown in [1, 2], the slope of the ocean bottom is able to capture the wave energy of the tsunami by tsunami refraction and directing the waves to the coastline. Usually, the ocean depth in the immediate vicinity of the island is significantly less than in the open ocean, although the cases of sharp depth growth directly from the coastline are not excluded. Further, we assume that the depth growth occurs quite gradually and the width of this bottom slope significantly exceeds the wavelength of the tsunami. Therefore, the rectilinear front of the tsunami wave while approaching the island undergoes significant distortions, which entails a tsunami attack on the island's coastline from almost all sides (not only from the initial tsunami moving direction). Given ratio between the bottom slope width and the wavelength allows using the ray approximation to study the wave refraction process.

This task was considered by many researchers, and there are a number of publications on this subject [3–5]. The process of transformation of an initially flat long wave approaching an axisymmetric (round) island using different method was investigated in [3], where for the case of a conical bottom relief an approximate analytical formulae for the amplitude of refracted waves were used. Here are the problem statement and some results of this work.

*This work was carried out under state contract with ICMMG SB RAS (0315-2019-0004).

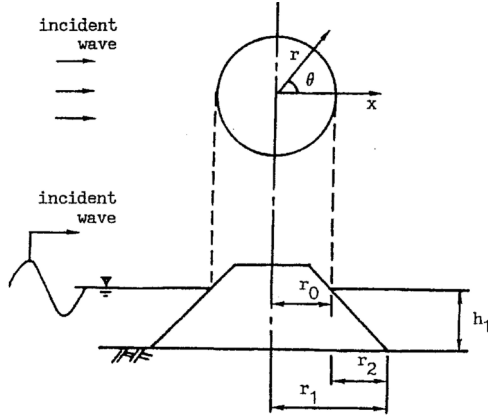


Figure 1. The scheme of wave refraction problem around a conical island [3]. Wave attacks island from the left side

Figure 1 (taken from [3]) schematically shows a conical island placed in an area with a constant depth, while in some vicinity of the island the depth increases linearly with distance from the coastline to a maximum h_1 value. A wave approaches this island from the left side, with the profile presented in the figure. The island edge line is a circle with a radius of r_0 , and the bottom slope ends at a distance r_2 from the center of the island. The θ angle expresses the azimuth as shown at the top ($\theta = 0$ is initial direction of wave motion).

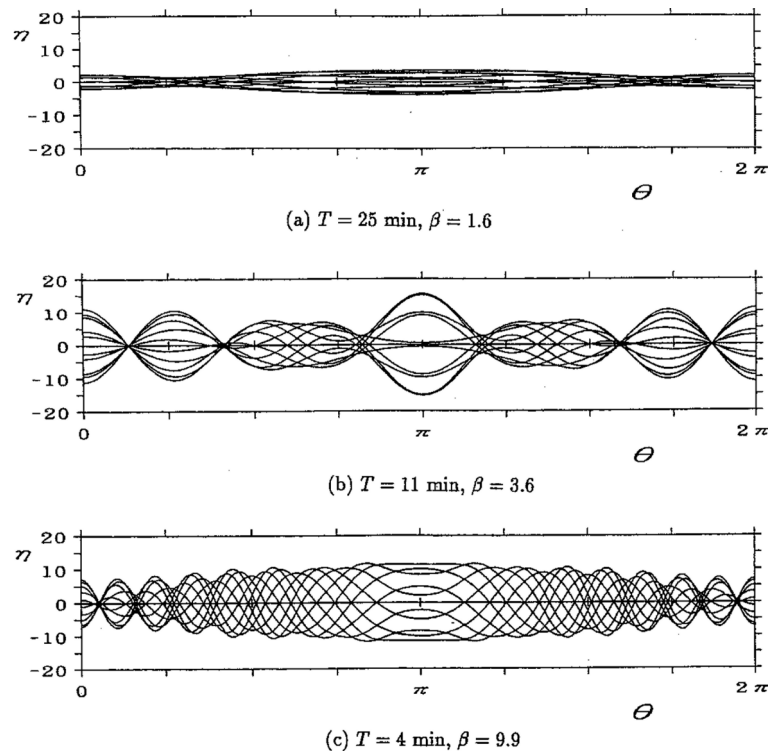


Figure 2. Distribution of wave heights along the perimeter of the island for different wavelengths [3]. The π angle corresponds to the front of the island

In the paper, using an approximate solution for harmonic waves, the state of the water surface for different wavelengths and times was found. At the same time, the hydraulic modeling of this problem was carried out in the water fume. Figure 2 (also taken from [3]) compares wave amplitudes along the island shoreline for different wavelengths and incident wave periods. Here, the β parameter is the inverse value to relative (normalized to the island radius) wavelength.

Local amplitude maxima in the frontal part of the coastline ($\theta = \pi$) and in the rear part ($\theta = 0$) are explained by reflection of oncoming wave and the collision of refracted waves just behind the island (Figures 2a, 2b). The direction of the wave front movement can be traced by wave rays constructed by numerical solution of differential equations for the wave ray (Figure 3).

The change in direction of the wave rays depends on the span of the slope for the near-island bottom and on the maximum depth. However, typically the rear part of island exhibits a collision of refracted waves that bypass the island from different sides. Figure 3 (also taken from [3]) shows the wave rays for the wave segment bypassing the island from below.

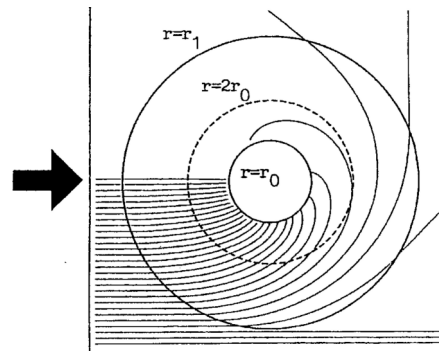


Figure 3. Refraction of wave rays over the bottom slope near an island surrounded by the conical bottom slope [3]

Consider the behavior of the wave front of the initially flat tsunami wave in the same setting of the problem as in [3]. Around a circular island with a radius of r_0 , the depth increases linearly from zero to a maximum value (at the distance r_1 from the island center). This relief is shown schematically in Figure 1. This problem was numerically solved using the method of step-by-step orthogonal advance of the wave front as described in [6].

2. Simulation of tsunami kinematics by wave front orthogonal advance method

Behavior of the wave front in two-dimension area can be described by the eikonal equation

$$|\nabla\tau|^2 = \frac{1}{c^2(x,y)}, \quad (1)$$

where $c(x,y)$ the wave velocity at a point (x,y) . The curve $\tau(x,y,x_0,y_0) = t$ describes a wave front at the time instance t , while x_0 and y_0 are the coordinates of the point source. Some properties of equation (1) are described in [7] where it was shown that for any velocity distribution in the medium,

the front points of the wave always move in an orthogonal direction to the front line with a velocity corresponding to the conductivity of the medium at a given point. In the case of tsunamis, this velocity depends only on the depth H and is determined by the Lagrange formula [8]

$$c = \sqrt{gH}. \quad (2)$$

Publication [7] also introduces a concept of wave rays, which are the curves orthogonal to the wave front all the time. These properties of wave fronts and rays are the basis for the numerical method of step-by-step orthogonal advancement of wavefront points; now we present a brief description of this method.

Consider a rectangular computation domain, where the wave propagation velocity $c(x, y)$, $0 < x < X_{\max}$, $0 < y < Y_{\max}$, is known for each point. In the case of a tsunami wave, its propagation speed can be calculated using the Lagrange formula (2) if the depth distribution is known. Consider the curve presenting the initial wavefront position. As a rule, closed convex curves will be taken as such. For example, a circle or an ellipse. Their smoothness is not required because in the numerical method, the starting front is a finite number of points located along this curve. Let us assume that the area bounded by this curve is the whole source of perturbations, that is, it is a source of tsunami. Therefore, the wave propagates in the direction of the external normal to this curve. Before starting numerical calculations, you need to select a time step that determines the time difference between each subsequent positions of the wave front. Obviously, the smaller this step, the more accurate is the result of numerical modeling, but this might increase the calculation time.

So, there is a finite set of points P_i with coordinates (x_i, y_i) , $i = 1, \dots, N$, located along the closed curve of the initial wave front. The point with index N is adjacent to the point with index 1. The value of the time step is Δt recommended to be chosen inversely to the maximum of the velocity gradient in the region under investigation. We need to determine the position where the initial wave front points will reach after the time step Δt . First, the direction of movement of each of the N calculated points is to be estimated. As already mentioned, the points will move orthogonally to the line of the current wave front. Since instead of a continuous smooth front we have a broken front passing through the points P_i , the desired orthogonal direction at a point with index i can be built in different ways. In the software implementation of this method, this direction is constructed as an external normal to a circle drawn through three points P_{i-1} , P_i and P_{i+1} . Thus, the next position of the calculated point with index i is determined by moving point P_i along the found direction by a distance $c(x_i, y_i)\Delta t$, where the speed $c(x_i, y_i)$ is determined by the Lagrange formula (2). In the case of a closed wave front line, the front line of the adjacent points for points

with indices 1 and N that used to construct the circle will be points P_N and P_1 , respectively. By moving all the points of the initial wave front in this manner, we can obtain a position of the wave front at the time Δt . Further, repeating this procedure until the wave front reaches the desired point or the computational area boundary, it is possible to build a kinematic picture of the tsunami wave propagation from an initial wave front in the area which surrounds the given source. If the calculated wave front is not closed, then the direction of starting and ending points movement is determined either as normal to the segment connecting this point with the nearest neighbor, or as a normal to the circle passing through the three first or tree last computation points on the wave front line. It should be noted here that according to the wave ray definition [7], the calculated front points will move along the wave rays.

A series of snapshots in Figures 4 shows the consecutive wave-front positions in the vicinity of a conical island. A smaller radius circle r_0 represents the shoreline, and a larger circle (with the radius r_1 by 3 times bigger than the island radius) represents the sloping bottom end, and the depth becomes constant.

Figure 4 shows that a part of wave front is captured by the sloping bottom and starts circulating around the island. At the same time, the wave amplitude weakens quite quickly due to a significant stretching of the front

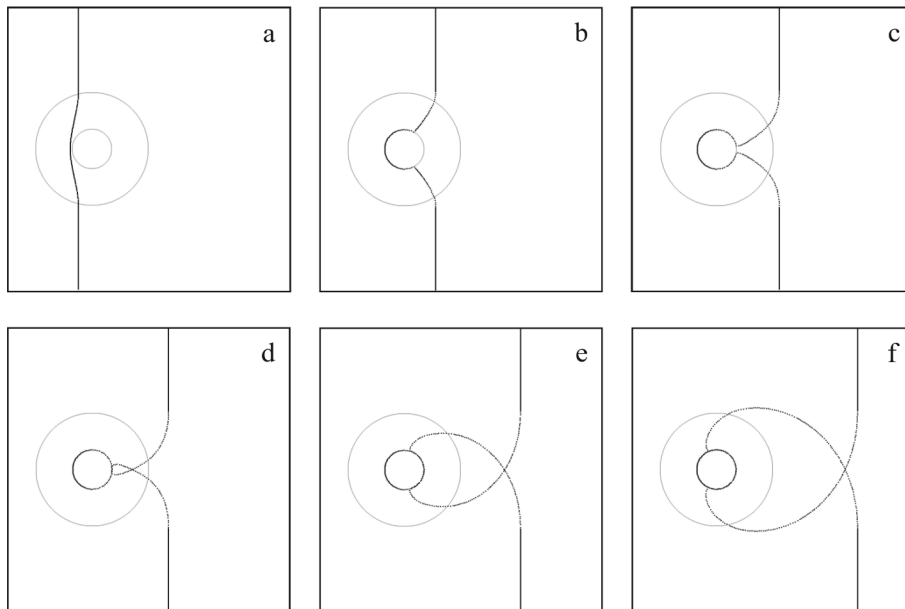


Figure 4. The sequential position of the initially straight wave front as it moves near a circle island surrounded by an inclined shelf

line near the coastline. The kinematic picture obtained by the numerical method shows that after the leading wave passes the island, we observe a second wave beyond the main wave with a lower amplitude. For the opposite direction (where the wave came from), at least one weak wave propagates due to wave reflection from the island. The second weak wave is generated by refraction and diffraction of the initial wave caused by the bottom slope around the island.

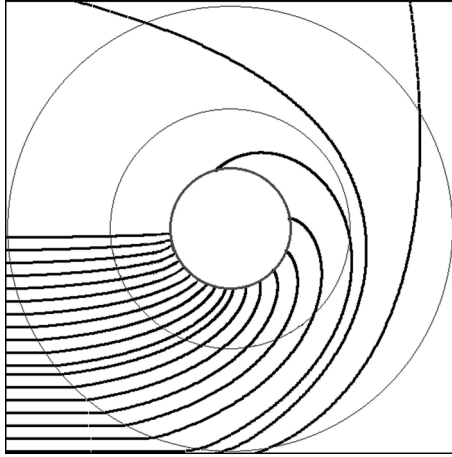


Figure 5. The wave-rays traces near the conical island, constructed by the method of step-by-step orthogonal advance of the wave front

By the same numerical method [6], wave ray trajectories during wave refraction over the bottom slope around the island were built. The results of simulation are shown in Figure 5. Here, gray circles mean the same as in Figure 3 taken from work [3]. It is not difficult to see a qualitative similarity of the wave ray behavior presented in these figures. The little mismatch is caused by a difference in depth values outside the bottom slope. This confirms again the reliability of the method for orthogonal advancement of wave front applied for solving kinematic problems of this kind.

3. Numerical modeling of wave dynamics near a round island

To quantify the value of the captured wave energy and tsunami parameters near the island, a computational experiment was carried out to simulate the behavior of a long wave near a conical island described earlier (see Figure 1). A tsunami wave with an initially rectilinear front line approaches a circular island schematically represented in Figure 1. Numerical model used here is based on a two-dimension system of nonlinear shallow-water equations [8] and the MOST difference scheme [9]. The initial wave is generated by the following boundary conditions:

$$\eta(1, j) = 0.5 \left(1 - \cos \frac{2\pi t}{T} \right), \quad u(1, j) = \eta(1, j) \sqrt{\frac{g}{D(1, j)}}, \quad v(1, j) = 0, \quad (3)$$

$$j = 1, \dots, 1600, \quad 0 \leq t \leq T.$$

Here η is the vertical surface displacement, u and v are the horizontal water flow velocity components, D is depth, g is gravity acceleration. The

height of the initial wave was taken equal to 100 cm and the period T was 300 s. The radius of the island is $r_0 = 100$ km, and the radius r_1 of the sloping bottom around the island is taken as 400 km (see Figure 1). Outside the shelf (at a distance of more than 400 km from the center of the island), the depth becomes constant and equal to 1000 m. The size of the computational grid is 1600×1600 knots with a spatial step of 1 km in both directions. The center of the island is situated at a distance 700 km from the left boundary and in the middle of domain for the vertical direction.

Figure 6 shows the water surface after the wave starts moving from the left boundary of the computational domain. Here, a smaller radius circle shows the shoreline of the island, and a larger radius circle (dashed line) denotes the edge of the bottom slope around the island.

The refraction of the wave front above the conical bottom slope is shown (limits are drawn with a white dashed line). As a result of refraction, the waves bend around the island on both sides and collide behind it. At the same time, the configuration of the wave front qualitatively coincides with the positions of the wave front in Figures 4a, 4c and 4d, although in that kinematic problem the radius r_1 was only 3 times larger than the radius of the island r_0 , and in this computational experiment we take $r_1/r_0 = 4$.

It can be seen from Figures 3, 4d, 5, 6b, and 6c that the wave energy that was contained in the initial wave segment having the width of about 3.5 bigger than the island diameter is captured by the bottom slope around the island. This reduces, respectively, the wave energy that continues moving towards the right border. Calculation of the wave energy contained at an area S of the computational domain was executed by the formula

$$E = \iint_S \left(\frac{\rho u^2}{2} (D + \eta) + \frac{\rho g \eta^2}{2} \right) ds, \quad (4)$$

where ρ is the liquid density, η is the wave height at the point under consideration, D is the depth, g is the acceleration of gravity, and u is the velocity of the water flow being constant from surface to bottom.

To illustrate the shielding ability of a conical island (together with the bottom slope), a distribution of tsunami height maxima for the entire course of computations is shown in Figure 7. A grey circle denotes the island, and a white dashed circle with a radius of 400 km limits the bottom slope around it. The “shadow” zone behind the island with maximum heights less than 40 cm is clearly visible, while its width is comparable to the diameter of the shelf around the island with the conical bottom topography. Along the central line of this zone, there is a local rise in the tsunami height maxima due to the collision of oncoming waves observed in Figures 4d and 6c.

The wave energy is estimated by formula (4) in the 300 km wide subarea along the left boundary and in the 400 km wide subarea near the right boundary. The first value E_1 corresponds to the energy of initial wave. The

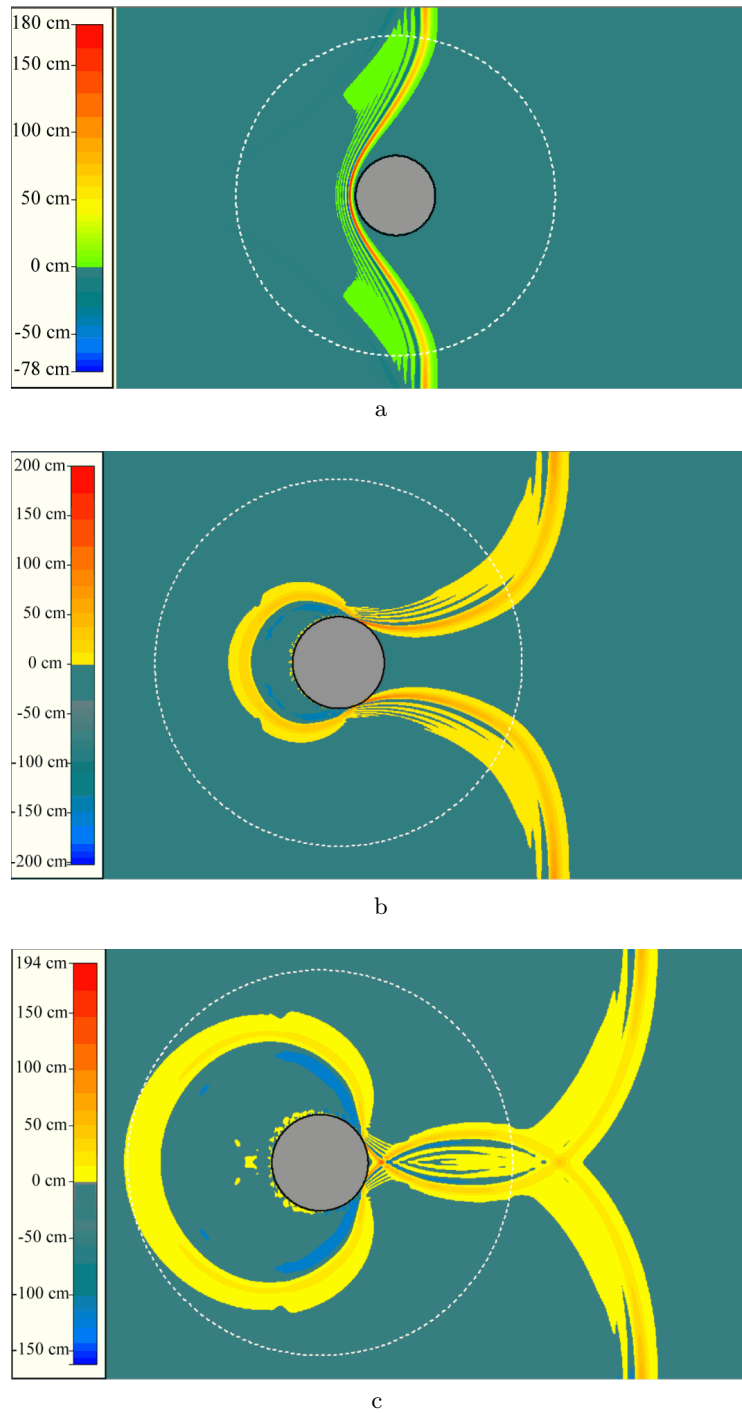


Figure 6. Water surface around an island 8,000 (a), 12,000 (b), and 14,000 (c) seconds after start of wave generating

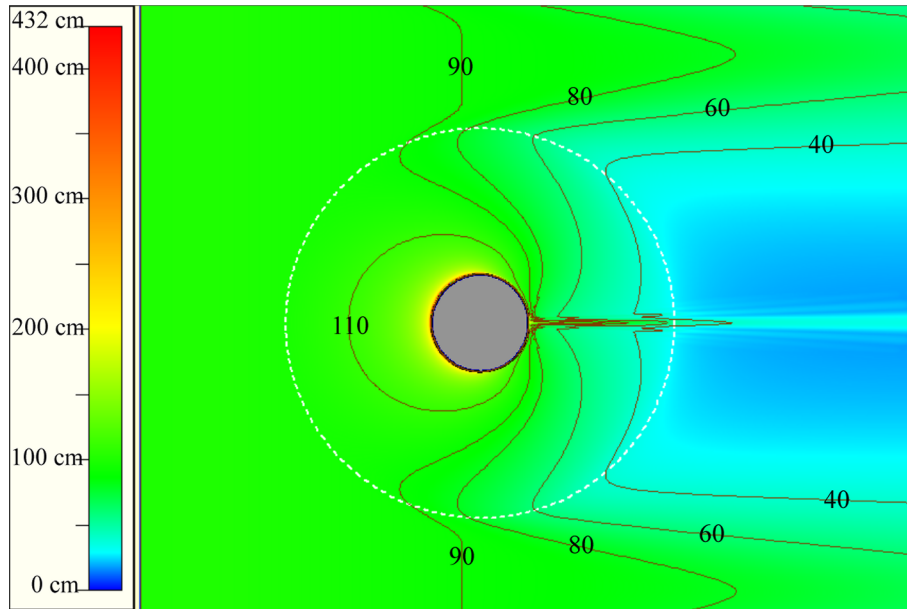


Figure 7. Distribution of the wave height maxima as the result of tsunami computation using the shallow-water model. Island drawn by grey color. The color to surface elevation legend is presented at the left side of figure

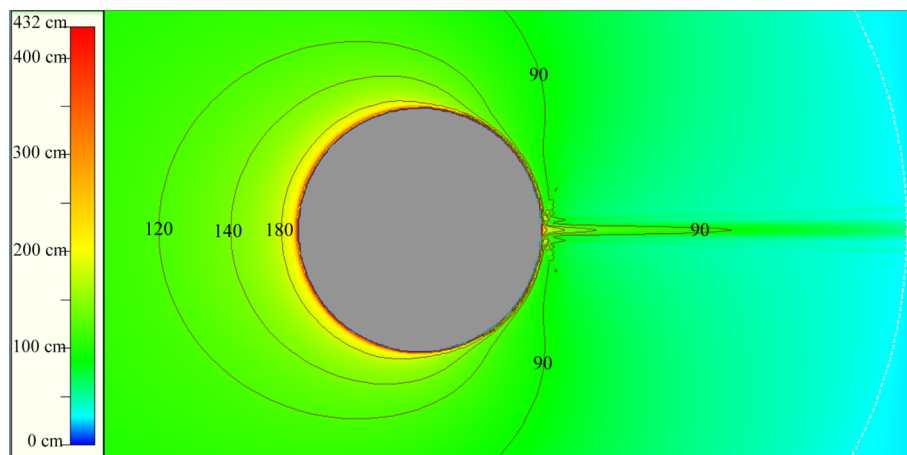


Figure 8. The more detailed view to the maximum wave height distribution around the island

second value E_2 gives the energy estimation for the wave after it passes island and its sloping shelf. The energy estimate showed that the decrease in energy ($E_1 - E_2$) of the exiting wave (through the right boundary) as compared to entering one is approximately equal to the energy in the segment of the original wave having the width equal to 3.4 diameters of the round island.

A more detailed distribution of the maximum tsunami heights near the island coastline can be seen in Figure 8, where the distribution shown in Figure 7 is visualized with greater details. It can be seen that the elevation distribution along the shoreline corresponds qualitatively to the distribution shown in Figure 2a.

Conclusion

The island, surrounded by a shelf with an inclined bottom, significantly affects the kinematics of the tsunami wave propagating in the area of the location of this island. Due to refraction over the sloping bottom around an island, the wave-front segment is strongly curving. Thus, the wave energy is redirected towards the coastline and the directions orthogonal to the initial wave movement direction. Numerical modeling of kinematics and dynamics of the wave with an initially rectilinear front line showed that after passing the island the loss in wave energy is equal to the energy of the wave segment having the width equal to approximately the diameter of the island's shelf zone. At the same time, a "shadow" zone with significantly smaller tsunami amplitude appears behind the island.

References

- [1] Marchuk An.G., Moskalensky E.D. Some analytical (exact) solutions for tsunami wave rays and front // Bull. Novosibirsk Comp. Center. Ser. Math. Mod. in Geoph.—Novosibirsk, 2010.— Iss. 13— P. 113–126.
- [2] Marchuk An.G. Benchmark solutions for tsunami wave fronts and rays. Part 1: Sloping bottom topography // Science of Tsunami Hazards.— 2016.— Vol. 35, No. 2.— P. 34–48.
- [3] Fujima K., Yuliadi D., Goto C., et al. Characteristics of long waves trapped by conical island // Coastal Engineering in Japan.— 1995.— Vol. 38, No. 2.— P. 111–132.
- [4] Jonsson I.G., Skovgaard O., Brink-Kjaer O. Diffraction and refraction calculations from waves incident on an island // J. Marine Res.— 1976.— Vol. 34, No. 3.— P. 469–496.
- [5] Lautenbacher C.C. Gravity waves refraction by islands // J. Fluid Mech.— 1970.— Vol. 41, Part 3.— P. 655–672.

-
- [6] Marchuk An.G., Vasiliev G.S. The fast method for a rough tsunami amplitude estimation // Bull. Novosibirsk Comp. Center. Ser. Math. Modeling in Geophysics. — Novosibirsk, 2014. — Iss. 17. — P. 21–34.
 - [7] Romanov V.G. Inverse Problems of Mathematical Physics. — Netherlands: VSP, 1984.
 - [8] Stocker J.J. Water Waves. The Mathematical Theory with Applications. — New York: Interscience Publishers, 1957.
 - [9] Titov V.V., Gonzalez F. Implementation and Testing of the Method of Splitting Tsunami (MOST). — Washington DC, 1997. — (Technical Memorandum / National Oceanic and Atmospheric Administration; ERL PMEL-112).

